

Synthesis and luminescence properties of $\text{Na}_3\text{Gd}(\text{PO}_4)_2 : \text{Dy}^{3+}$ phosphors

Jae Jeong Shim^a, Misun Jo^{a,b}, B.C. Jamalajah^a, Jiang Zehan^a, Sun Il Kim^{a,*}, Wan Young Chung^b and Hyo Jin Seo^{a,*}

^aDepartment of Physics and Interdisciplinary Program of Biomedical, Mechanical & Electrical Engineering, Pukyong National University, Busan 608-737, Korea

^bDepartment of Electronic Engineering, Pukyong National University, Busan 608-737, Korea

Dy³⁺-doped $\text{Na}_3\text{Gd}(\text{PO}_4)_2$ phosphors were synthesized by high temperature solid-state reaction. The X-ray diffraction patterns and Fourier transform infrared absorption measurements were performed to characterize the synthesized phosphors. The excitation and emission spectra of Gd^{3+} and Dy^{3+} in $\text{Na}_3\text{Gd}(\text{PO}_4)_2 : \text{Dy}^{3+}$ were detected in the wavelength region from UV to visible. With increasing Dy^{3+} concentration, the Gd^{3+} emission at 313 nm due to the ${}^6\text{P}_{7/2} \rightarrow {}^8\text{S}_{7/2}$ transition decreases, while blue and green emissions due to the $\text{Dy}^{3+} \rightarrow {}^4\text{F}_{9/2}$ ${}^4\text{H}_{15/2, 13/2}$ transitions increase under excitation into the $\text{Gd}^{3+} {}^6\text{I}_{7/2}$ Level. The results indicate that the efficient energy transfer occurs from Gd^{3+} to Dy^{3+} in $\text{Na}_3\text{Gd}(\text{PO}_4)_2 : \text{Dy}^{3+}$.

Key words: luminescence, Gd^{3+} ions, Dy^{3+} ions, Energy transfer, Phosphates, $\text{Na}_3\text{Gd}(\text{PO}_4)_2$

Introduction

In recent years the luminescence properties of rare earth ions doped in Gd-based compounds were extensively studied in spectral region from vacuum ultraviolet (VUV) to visible not only from the practical viewpoint of quantum cutting phosphors, but also for the purpose of scientific interest [1-5]. However, energy transfer and relaxation processes in these materials have not well been understood. The study on relaxation processes makes the optimization of the phosphor performances possible. Double phosphates of the type $\text{Na}_3\text{Ln}(\text{PO}_4)_2$ (Ln = La-Tb) crystallize orthorhombic (SG Pbc2₁; Z = 24); they are built up on isolated LnO_7 decahedra and PO_4 tetrahedra [6]. Considering ionic radii and valence state the Dy^{3+} ions substitute for Gd^{3+} sites in $\text{Na}_3\text{Gd}(\text{PO}_4)_2$. The compounds of phosphates doped with rare-earth ions have been investigated as promising phosphors for white light-emitting diodes (LEDs) and plasma display panels [7-11]. Recently several groups have studied the spectroscopic properties of $\text{Na}_3\text{Gd}(\text{PO}_4)_2 : \text{Ln}^{3+}$ (Ln = Ce, Eu, Tb) in the VUV-visible region [9-11]. However, no details in energy transfer process in $\text{Na}_3\text{Gd}(\text{PO}_4)_2 : \text{Dy}^{3+}$ has been reported. In this paper we report energy transfer between the host self-trapped exciton (STE) state and the Gd^{3+} , Eu^{3+} ions and relaxation processes in the VUV-visible region under excitation into the STE state in $\text{Ca}_3\text{Gd}_2(\text{BO}_3)_4 : \text{Eu}^{3+}$.

Experimental

$\text{Na}_3\text{Gd}(\text{PO}_4)_2$ phosphors containing Dy^{3+} ions were

synthesized by solid-state reaction technique using Na_2CO_3 (99.9%), $\text{NH}_4\text{H}_2\text{PO}_4$ (99.9%), Gd_2O_3 (99.99%), Dy_2O_3 (99.99%) as raw materials. The crystallization and phase transformation temperatures were obtained from thermo-gravimetric differential-thermal analysis (TG/DTA) of the precursor with a Material Analysis and Characterization TG-DTA 2000 at a heating rate of 5 °C/min. The stoichiometric homogeneous mixtures obtained by thorough grinding in the presence of acetone were fired at a heating rate of 2 °C/min in two steps at 200 and 400 °C for 3 hr and then sintered at different temperatures (from 700 to 1000 °C) for 3 hr in air. The phase purity of the samples were identified through XRD analysis using X'Pert PRO X-ray diffractometer with CuK_α (1.5406 Å) radiation source. The Fourier transform infrared (FTIR) absorption spectrum of the $\text{Na}_3\text{Gd}(\text{PO}_4)_2$ sintered at 900 °C/3 h was recorded with a Spectrum-GX spectrophotometer by KBr pellet method. The excitation and emission measurements were taken with a Photon Technology International fluorimeter with xenon flash lamp (60 W) as a light source. The pulsed excitation source for decay measurements was 4th harmonics (266 nm) of Nd: YAG laser (SL802G) equipped with Acton Research Corp. Pro-750 monochromator. Decay profiles were recorded with a Tektronix DPO 3054 digital storage oscilloscope in which the signal was fed from PMT (Hamamatsu R928). All the measurements were carried out at room temperature.

Results and Discussion

Thermal analysis

Fig. 1 shows the TG-DTA curves of the $\text{Na}_3\text{Gd}(\text{PO}_4)_2$ precursor. The TG curve (Fig. 1(a)) exhibits two weight loss steps in the temperature region 25-500 °C.

*Corresponding author:

Tel : +82-51-629-5568

Fax: +82-51-629-5549

E-mail: hjseo@pknu.ac.kr (H.J. Seo), sikim@pknu.ac.kr (S.I. Kim)

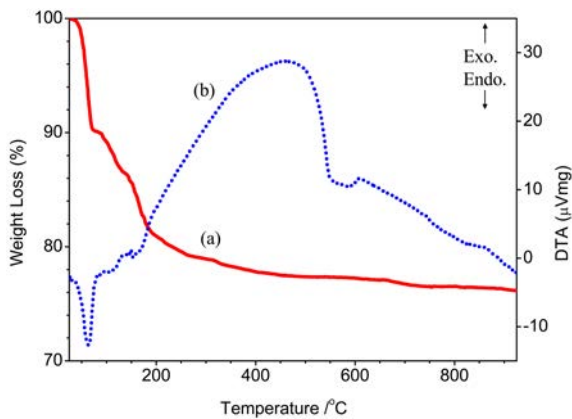


Fig. 1. (a) TG and (b) DTA curves of $\text{Na}_3\text{Gd}(\text{PO}_4)_2$ precursor.

With increasing temperature, the weight loss occurs up to 500 °C thereafter no weight loss occurs indicating the decomposition of all organic groups present in the precursor. The endothermic peak at around 65 °C is due to the evaporation and oxidation of OH and organic groups. In the course of evaporation the weight loss is of about 10%. However, the total weight loss is found to be only about 22.6%. The exothermic reaction (Fig. 1(b)) takes place between 150-550 °C accompanied with the most significant weight loss which is attributed to the decomposition of organic groups present in the precursor. The exothermic peak at 610 °C is connected to the phase transition of $\text{Na}_3\text{Gd}(\text{PO}_4)_2$. However, the reaction threshold temperature is found to be 900 °C for a typical orthorhombic structure.

XRD and FTIR spectroscopy

In order to optimize the sintering temperature of $\text{Na}_3\text{Gd}(\text{PO}_4)_2$, the powder obtained at 400 °C was fired at different temperatures of 700, 800, 900 and 1000 °C for 3 hr. The XRD profiles of these samples are illustrated in Fig. 2. The XRD peaks obtained at 900 °C are well consistent with the standard JCPDS#29-1208 data for a typical orthorhombic structure with space group $Pcmb$ and cell parameters: $a = 5.299$, $b = 18.376$ and $c = 13.878$ (Å). The XRD patterns reveal the same phase for Dy^{3+} -doped $\text{Na}_3\text{Gd}(\text{PO}_4)_2$. The FTIR spectrum of $\text{Na}_3\text{Gd}(\text{PO}_4)_2$ sintered at 900 °C/3 hr is shown in Fig. 3. The assignment of IR absorption bands have been done following the literature [12-14]. Generally, the orthophosphates contains $(\text{PO}_4)^{3-}$ units whose site symmetry depend on the structure of the orthophosphate. Moreover, the IR absorption band of $(\text{PO}_4)^{3-}$ has four normal modes of vibrations ν_1 (~990-1010 cm^{-1}), ν_2 (~600 cm^{-1}), ν_3 (~1040-1100 cm^{-1}) and ν_4 (~630 cm^{-1}). The most intense vibration (ν_1) represents the P-O displacement (totally symmetric), the ν_2 and ν_4 vibrations are due to the deformation angle modes and ν_3 vibration represents the anti-symmetric displacement of PO_4 compound. The IR bands at 1740 and 1586 cm^{-1} are due to the free

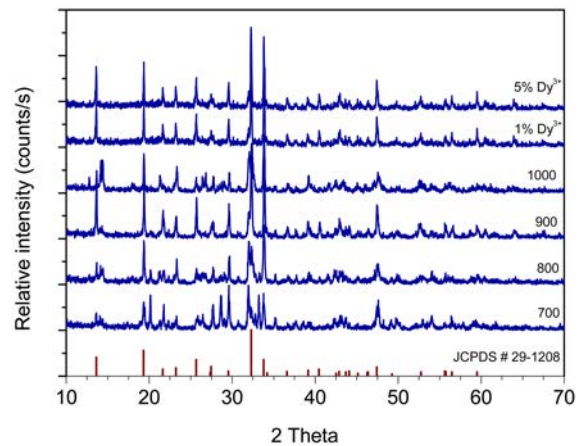


Fig. 2. XRD profiles of undoped $\text{Na}_3\text{Gd}(\text{PO}_4)_2$ at different temperatures and Dy^{3+} -doped $\text{Na}_3\text{Gd}(\text{PO}_4)_2$ sintered at 900 °C/3 hr.

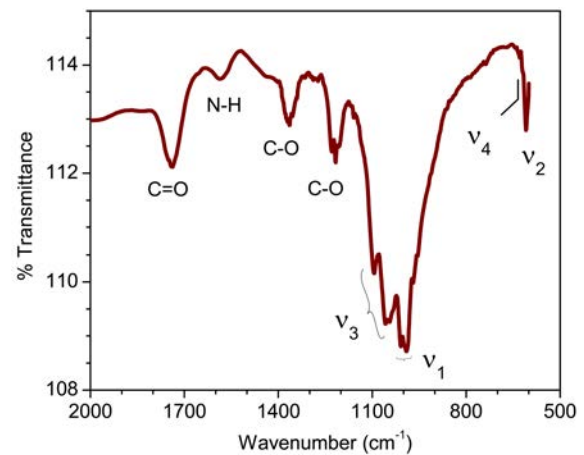


Fig. 3. The FT-IR spectrum of undoped $\text{Na}_3\text{Gd}(\text{PO}_4)_2$ sintered at 900 °C/3 hr.

carbonyl group (C = O) and bending vibrations of N-H group, respectively. The absorption bands at 1366 and 1263 cm^{-1} are attributed to C-O stretching vibrations.

Excitation and emission spectra of $\text{Na}_3\text{Gd}(\text{PO}_4)_2 : \text{Dy}^{3+}$

The excitation spectrum of $\text{Na}_3\text{Gd}(\text{PO}_4)_2 : \text{Dy}^{3+}$ (1.0 mol%) obtained by monitoring the emission at 575 nm ($\text{Dy}^{3+} \rightarrow {}^4\text{F}_{9/2} \text{ } {}^6\text{H}_{13/2}$) is shown in Fig. 4. The excitation lines at 250, 275 and 313 nm are attributed to the $\text{Gd}^{3+} \text{ } {}^8\text{S}_{7/2} \text{ } {}^6\text{D}_J$, ${}^6\text{I}_J$, ${}^6\text{P}_J$ transitions, respectively. The lines at 296, 326, 340, 352, 366, 388, 428, 450 and 473 nm are assigned to the ${}^6\text{H}_{15/2} \rightarrow {}^4\text{F}_{3/2}$, ${}^6\text{P}_{3/2}$, (${}^4\text{F}$, ${}^4\text{D}$) $_{5/2}$, ${}^6\text{P}_{7/2}$, ${}^6\text{P}_{5/2}$, ${}^4\text{F}_{7/2}$, ${}^4\text{G}_{11/2}$, ${}^4\text{I}_{15/2}$ and ${}^4\text{F}_{9/2}$ transitions of Dy^{3+} , respectively. The energy transfer from Gd^{3+} to Dy^{3+} is responsible for the appearance of Gd^{3+} -excitation lines for the Dy^{3+} emission. One notes that the strongest excitation line is observed at 275 nm due to the $\text{Gd}^{3+} \text{ } {}^8\text{S}_{7/2} \rightarrow {}^6\text{I}_J$ transition.

Fig. 5 shows the emission spectra of $\text{Na}_3\text{Gd}(\text{PO}_4)_2 : \text{Dy}^{3+}$ (0.1 and 5 mol%) under 275 nm ($\text{Gd}^{3+} : {}^8\text{S}_{7/2} \rightarrow {}^6\text{I}_J$) excitation. The emission spectra exhibit a total of three emission bands centered at 313 nm ($\text{Gd}^{3+} :$

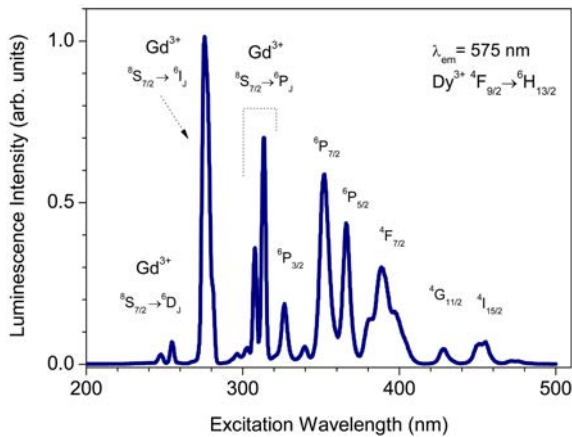


Fig. 4. The excitation spectrum of $\text{Na}_3\text{Gd}(\text{PO}_4)_2 : \text{Dy}^{3+}$ (1%) obtained by monitoring the 575 nm emission due to the ${}^4\text{F}_{9/2} \rightarrow {}^6\text{H}_{13/2}$ transition.

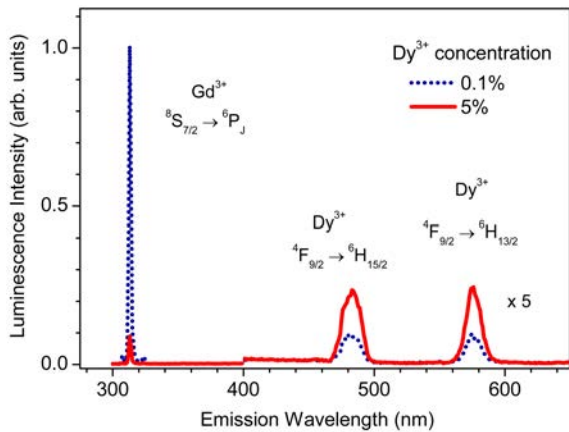


Fig. 5. The emission spectra of $\text{Na}_3\text{Gd}(\text{PO}_4)_2 : \text{Dy}^{3+}$ (0.1 and 5%) under excitation into the $\text{Gd}^{3+} {}^6\text{I}_1$ state at 275 nm.

${}^6\text{P}_{7/2} \rightarrow {}^8\text{S}_{7/2}$, 484 nm ($\text{Dy}^{3+}: {}^4\text{F}_{9/2} \rightarrow {}^6\text{H}_{15/2}$) and 575 nm ($\text{Dy}^{3+}: {}^4\text{F}_{9/2} \rightarrow {}^6\text{H}_{13/2}$). It is clear that the emission intensity of Gd^{3+} decreases with increasing Dy^{3+} concentration but does not completely disappear even for 5% of Dy^{3+} . The intensity of Dy^{3+} increases with increasing Dy^{3+} concentration. This is attributed to higher absorption cross section for higher Dy^{3+} concentration as well as a well-known phenomenon of energy transfer from Gd^{3+} to Dy^{3+} . As shown in Fig. 6, the 275 nm UV light excites the $\text{Gd}^{3+} ({}^8\text{S}_{7/2})$ ions into the excited state of $\text{Gd}^{3+} {}^6\text{I}_1$ followed by nonradiative relaxation to the ${}^6\text{P}_{7/2}$ state. The emissions occur at 313 nm (Gd^{3+}) and 484 + 575 nm (Dy^{3+}) by the two channels, i.e., direct transition to the $\text{Gd}^{3+} {}^8\text{S}_{7/2}$ state and energy transfer from $\text{Gd}^{3+} {}^6\text{P}_{7/2}$ to $\text{Dy}^{3+} {}^6\text{P}_{3/2}$. The relaxation from $\text{Dy}^{3+} {}^6\text{P}_{3/2}$ to $\text{Dy}^{3+} {}^4\text{F}_{9/2}$ through nonradiative process is followed by the 484 nm (blue) and 575 nm (green) emissions. For higher Dy^{3+} concentration an efficient energy transfer from Gd^{3+} to Dy^{3+} occurs because the average distance between Gd^{3+} and Dy^{3+} is shorten.

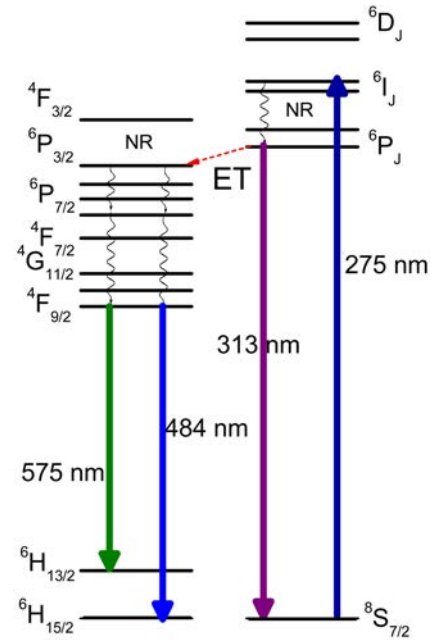


Fig. 6. Schematic showing the excitation into the $\text{Gd}^{3+} {}^6\text{I}_1$ state, the relaxation to the excited ${}^6\text{P}_{7/2}$ state of Gd^{3+} and energy transfer to the $\text{Dy}^{3+} {}^6\text{P}_{3/2}$ state, the emissions from ${}^6\text{P}_{7/2}$ to ${}^8\text{S}_{7/2}$ (313 nm) and from ${}^4\text{F}_{9/2}$ to ${}^6\text{H}_{13/2}$ (575 nm), ${}^6\text{H}_{15/2}$ (484 nm).

Conclusions

The luminescence properties under excitation into the $\text{Gd}^{3+} {}^6\text{I}_1$ state are investigated in the Gd-based host of $\text{Na}_3\text{Gd}(\text{PO}_4)_2 : \text{Dy}^{3+}$. We observe the emission at 313 nm due to the $\text{Gd}^{3+} {}^6\text{P}_{7/2} \rightarrow {}^8\text{S}_{7/2}$ transition and the emissions at 484 and 575 nm due to the transitions from the ${}^4\text{F}_{9/2}$ state to the ${}^6\text{H}_{15/2}$, ${}^6\text{H}_{13/2}$ states of Dy^{3+} , respectively. It is found that the excited $\text{Gd}^{3+} {}^6\text{I}_1$ state transfers its energy efficiently to the $\text{Dy}^{3+} {}^4\text{F}_{9/2}$ state for the sample with higher Dy^{3+} concentration. We believe that such an analysis of luminescence relaxation processes will contribute to make the optimization of the phosphor performances possible, especially, for the Gd-based phosphors.

Acknowledgments

This work was supported by a Research Grant of Pukyong National University (2014).

References

1. X. Qio and H.J. Seo, *Mater. Res. Bull.* 49 (2014) 76-82.
2. X. Qio and H.J. Seo, *J. Lumin.* 145 (2014) 312-317.
3. X. Zhang, F. Meng, W. Li, S.I. Kim, Y.M. Yu, and H.J. Seo, *J. Alloys Compd.* 578 (2013) 72-76.
4. L. Qin, D. Wei, Y. Huang, S.I. Kim, Y.M. Yu, and H.J. Seo, *J. Nanopart. Res.* 15 (2013) 1940-1947.
5. Y. Huang, Y. Nakai, T. Tsuboi, H.J. Seo, *Opt. Express* 19 (2011) 6303.
6. M. Kloss, B. Finke, L. Schwarz, and D. Haberland, *J.*

- Lumin. 72-74 (1997) 684-686.
7. H.J. Seo, J. Ceram. Process. Res. 14 (2013) s22-s25.
 8. X. Qio and H.J. Seo, J. Ceram. Process. Res. 14 (2013) s30-s34.
 9. D. Wang, Y. Wang, and J. He, Mater. Res. Bull. 47 (2012) 142-145.
 10. H. Liang, Z. Tian, H. Lin, M. Xie, G. Zhang, P. Dorenbos, and Q. Su. Opt. Mater. 33 (2011) 618-622.
 11. G. Ju, Y. Hu, L. Chen, X. Wang, Z. Mu, H. Wu, and F. Kang, J. Alloys Compd. 509 (2011) 5655-5659.
 12. S. Hachani, B. Moine, A. El-akrmi, and M. Ferid, Opt. Mat. 31 (2009) 678-684.
 13. Y.H. Zhou, J. Lin, S.B. Wang, and H.J. Zhang, Opt. Mater. 20 (2002) 13-20.
 14. M. Kizilyalli, A. Sungur, D.S. Jones, J. Less-Comm. Metals 110 (1985) 249-254.